Magnetic focusing in parallel quantum point contacts

T. M. Eiles, J. A. Simmons, M. E. Sherwin, and J. F. Klem
Sandia National Laboratories, Albuquerque, New Mexico 87185
(Received 4 May 1995)

Using an air-bridged gate, we have fabricated two closely spaced parallel quantum point contacts (QPC's) in a GaAs-$Al_xGa_{1-x}As$ heterostructure. By biasing the gates appropriately, we have measured the magnetoresistance (MR) at low fields for both single and parallel point contacts. Assuming a parabolic potential, the MR of a single QPC can be quantitatively understood by a previous theory incorporating magnetic-field-suppressed backscattering. However, the MR of two QPC's in parallel displays resistance peaks, implying a failure of Ohm's law due to coupling between the channels. These resistance peaks are shown to be due to magnetic focusing of electrons from one channel into the other.

Ballistic electron transport can occur within devices smaller than the electron mean free path, and is a particularly simple regime in which to study electron coherence phenomena. The simplest ballistic device is the quantum point contact (QPC), a narrow constriction patterned in a two-dimensional (2D) electron gas (2DEG) whose width is on the order of the Fermi wavelength and whose length is shorter than the mean free path, so that it must be treated as an electron waveguide supporting a number of lateral one-dimensional modes. Several experimental configurations have exhibited such coherence phenomena as quantized conductance and electron-beam collimation.[1] However, semiclassical arguments not involving the wave nature of electronic motion can be used to interpret much of the data. For example, the magnetoresistance (MR) of a single QPC was interpreted by a semiclassical theory to adduce various features of the QPC's potential profile. In addition, magnetic focusing, a classical effect, has been observed in devices in which QPC's inject and collect electrons moving in cyclotron orbits.[2]

In this paper we discuss magnetotransport measurements of a system of two closely spaced parallel QPC's separated by a tunable potential maximum, or antidot, created by an independently biased center gate (Fig. 1). This system has been used to study resonant tunneling between edge states in the high-field quantum Hall regime,[3] and also the parallel addition of QPC conductances at zero field.[4] We focus in this work, however, on the semiclassical ballistic regime at low magnetic fields. Though the low-field MR data for single constrictions are well described by present theory, we find that the data for two parallel QPC's depart significantly from Ohm's law. MR peaks are found corresponding to a focusing of electron paths from one constriction to the other around the center antidot gate. While earlier work did find structure in the MR related to classical cyclotron orbits, the structures were either two-dimensional antidot arrays[5] or linear arrays of multiple closely spaced QPC's fabricated by focused ion beams[6] and therefore did not allow the antidot potential to be tuned independently of the adjacent QPC parameters, nor the individual QPC's to be characterized. Here we present MR focusing data, taken over a broad range of gate bias parameters, for a single tunable antidot bounded by two independently tunable and well-characterized QPC's. This enables us to observe the evolution of MR peaks with changing antidot potential, which is found to be consistent with independent measurements of the gate-induced edge depletion.

We fabricated the samples from two standard GaAs heterostructures: sample A with mobility $\mu=800\,000$ $cm^2/V\,s$ and two-dimensional electron density $n_{2D}=1.2\times10^{11}$ cm^{-2} and sample B with $\mu=10^6$ $cm^2/V\,s$ and $n_{2D}=2.0\times10^{11}$ cm^{-2}. The center gate (0.3 μm diam) drops from an air bridge suspended over both side gates, allowing separate bias voltages V_i $(i=1-3)$ to be applied to each of the gates. Fabrication details have been published elsewhere.[7] ac current (0.3–3 nA) is driven through the device, and the bulk Hall resistance R_H and the four-terminal longitudinal resistance R_L are measured by a low-frequency lock-in technique.

In Fig. 2 we show the low-field four-terminal magnetoresistance of a single point contact for a series of gate voltages. In our measurements of conductance vs gate voltage at $B=0$, only during a fraction of temperature cyclings were we able to observe well-defined steps. This

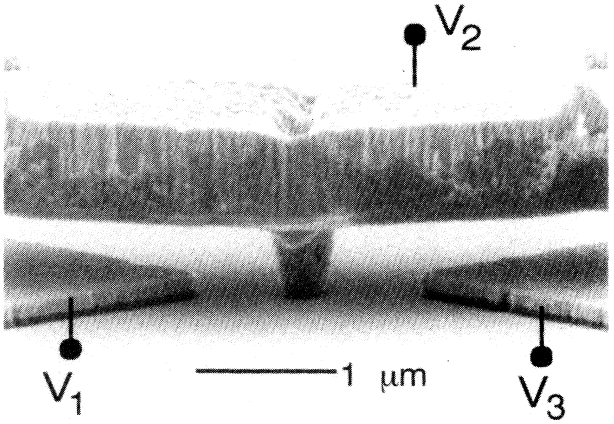

FIG. 1. SEM photograph of the airbridge structure and split gates used to define the two point contacts. Numbered voltages are applied to the gates as indicated. The lithographic width of the 2DEG channels on either side of the center gate is 0.8 μm.

0163-1829/95/52(15)/10756(4)/$06.00

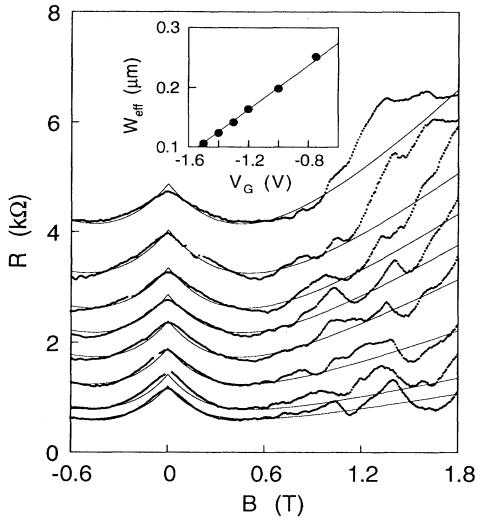

FIG. 2. Series of low-field magnetoresistance scans (sample B) for a single quantum point contact taken at $T=0.3$ K (thick lines). Voltages applied (in V) were $V_1=-3.2$, $V_2=-2.7$, and $V_3=-0.5$, -0.75, -1.0, -1.2, -1.3, -1.4, -1.5, and -1.6. Thin lines are fits to Eq. (1) assuming a parabolic potential for the point contact. Inset: Effective channel width as a function of gate voltage, obtained using the characteristic frequency and the 1D density parameters obtained in the fits.

is probably due to backscattering from impurities or dopant potentials in the fairly long (>0.5 μm) constrictions formed by the gate depletion.[8] The MR is characteristically negative at the lowest fields, becoming positive at a crossover point B_c. The resistance drop at the lowest fields was observed by van Houten *et al.*, and was explained in terms of suppressed backscattering due to localization of the electron cyclotron orbits near the sample walls.[9] This behavior can be understood quantitatively by the four-terminal resistance formula,

$$R_L=\frac{h}{2e^2}\left[\frac{1}{N_{\rm pc}(B)}-\frac{1}{N_{\rm bulk}(B)}\right]. \tag{1}$$

Both the number of transmitting bulk channels $N_{\rm bulk}=(h/2e)n_{\rm 2D}/B$ and the number of channels in the point contact $N_{\rm pc}(B)$ can be treated as continuous classical variables in the low-field regime we discuss here. The evolution of the number of channels in the constriction with B depends on the nature of the confinement potential, and has been calculated for both hard-wall and parabolic confinement potentials. Simulations of narrow split gate point contacts yield potentials that are more or less flat bottomed in the case of wide constrictions, but which evolve into more parabolic shapes as the constriction is narrowed.[10]

For a hard-wall potential, the number of channels in the constriction does not vary much if $B<B_c$, so the (negative) slope of the MR is basically the same as that of the Hall resistance ($1/en_{\rm 2D}$). Because the crossover field B_c increases as the point contact width is decreased, the magnitude of the resistance drop increases with negative bias. In contrast to previous work, our data do not demonstrate this trend; in fact, the net drop in resistance decreases slightly as the QPC is closed. The solution to this discrepancy is in a more accurate modeling of the QPC as a parabolic potential. We find that all our curves are best fit by the parabolic confinement model. In this model, the important parameters are the one-dimensional electron density $n_{\rm 1D}$ and the characteristic frequency of the parabolic potential Ω. The number of populated channels is given by

$$N_{\rm pc}(B)=\left[\frac{3\pi}{4}n_{\rm 1D}\left[\frac{\hbar}{2m^*\Omega}\right]^{1/2}\right]^{2/3}\frac{1}{\sqrt{[1+(\alpha B)^2]}}, \tag{2}$$

where $\alpha=e/m^*\Omega$.[11] The solid lines in Fig. 2 are fits to Eq. (1) using the measured bulk $n_{\rm 2D}$, and with $n_{\rm 1D}$ and Ω as fitting parameters.

It is possible[11] to define an effective QPC width

$$W_{\rm eff}=\frac{n_{\rm 1D}}{n_{\rm 2D}^{\rm QPC}} \tag{3}$$

using the 2D density in the constriction $n_{\rm 2D}^{\rm QPC}$. Following Berggren, Roos, and van Houten we compare Eq. (2) in the high-field ($\alpha B\gg 1$) limit with the filling factor in the constriction written in terms of the two-dimensional density: $N_{\rm pc}=(h/2e)n_{\rm 2D}^{\rm QPC}/B$. Comparing Eqs. (2) and (3) yields the effective width

$$W_{\rm eff}=2\pi n_{\rm 1D}^{1/3}\left[\frac{2\hbar}{3\pi m^*\Omega}\right]^{2/3}. \tag{4}$$

In the inset we show a plot of the calculated effective width derived from the fitting parameters as a function of the gate voltage applied. The dependence is linear, with the result that the width decreases by about 0.2 μm/V with the applied voltage, in good agreement with the depletion data. Recently, several theories have predicted various approaches to understanding the potential profile,[12] and we suggest that MR measurements may play a future role in better understanding the point-contact potential.

In Fig. 3 we show low-field MR data for *two* parallel point contacts for a series of different center gate voltages with the outer gate voltages held constant, so that both contacts are being narrowed simultaneously as the area of the center antidot is increased. Instead of the smooth MR curve of the single point contact, resistance peaks appear at low magnetic fields ($B<100$ mT). The peaks do not appear at all unless there is depletion under the center gate (data from second-to-lowest curve), which divides the channel into two separate QPC's. They begin to disappear again as the constrictions are made very narrow (data not shown). The peak positions do not change appreciably as a function of the center gate voltage. They are symmetric in magnetic field, and not part of a periodic oscillation, making it doubtful that their origin is due to quantum interference. They also persist to $T=4$ K. These peaks are a clear departure from Ohm's law, which would combine the MR curves for two paral-

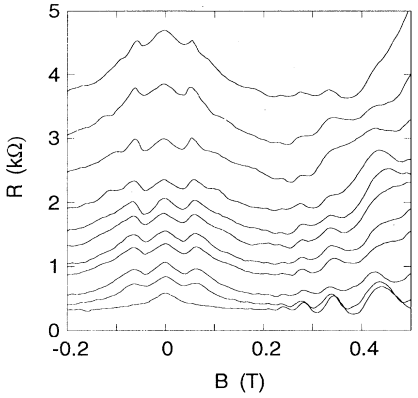

FIG. 3. Resistance vs magnetic-field curves for parallel point contacts in sample A. The side gates were set at $V_1 = V_3 = -0.8$ V, and the center gate voltage was stepped at V_2 (in V) = 0, −0.5, −0.9, −1.4, −1.6, −1.8, −1.9, −2.1, −2.3, −2.4, and −2.5.

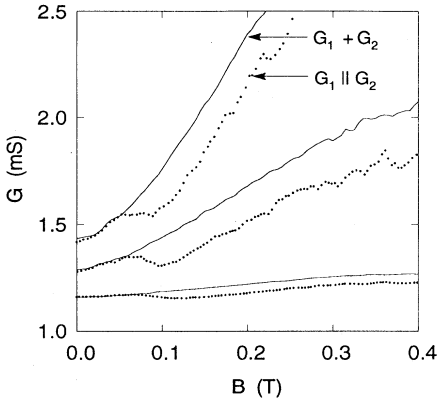

FIG. 4. Low-field magnetoconductance scans at three bias conditions of the two QPC's of sample B measured in parallel (dots), along with the *sum* of the conductances of the two QPC's measured individually (solid line).

lel QPC's, yielding a smooth MR with the same shape as the single OPC MR. As such, the peaks must be due to coupling between the conduction channels in the two QPC's. MR peaks related to trapped cyclotron orbits have been reported in antidot arrays and the resistance peaks we see are reminiscent of these.[5] Using $k_F = (2\pi n_{2D})^{1/2}$ and the measured peak position of 60 mT, we find a cyclotron radius $R_c = \hbar k_F / eB = 0.8$ μm, which is consistent with the lithographic dimensions and the smooth parabolic potential indicated by our data from a single QPC. The constancy of the peak position for all gate voltages seems surprising, at least when the constriction potential is thought of as bounded by hard walls that move laterally as the split gates deplete the 2DEG. However, as seen in the single-channel data, the low density of our samples yields a parabolic potential that gradually rises up to the Fermi level as the gate voltage is increased. The electrons are thus mostly emitted from the center of the constriction, which remains at a fairly constant position.

The above discussion can be quantified by first observing exactly how Ohm's law for combining the two resistances is circumvented in this geometry. This was done by taking MR curves for the parallel QPC configuration, then pinching off the two point contacts in succession and measuring the two individual single QPC MR scans. In Fig. 4 we show the magnetoconductance (MC) for three bias conditions. The large dots are the MC for the parallel case, displaying the conductance dip corresponding to the focused orbit. The lines are the sum of the conductances for the constituent point contacts. A small offset was added to make the curves coincide at $B = 0$; this accounts for the unavoidable effect that pinching off one side of the device has on the other side. The double QPC conductance drops at low fields, and then follows the shape of the single QPC combination, though there is a fairly constant conductance deficit that persists to higher B. The data indicate that at field well below the focusing peak, the two QPC's allow independent electron transport.

Further evidence of electron focusing can be seen in the data plotted in Fig. 5, where the side gates have been carefully balanced to give each of the constrictions the same width. Another set of peaks lies beyond the primary focusing peaks, becoming more prominent as the QPC's are narrowed. In contrast to the primary focusing peak, the position of these secondary peaks decreases substantially with negative center gate voltage. This secondary peak is suggestive of a magnetically focused

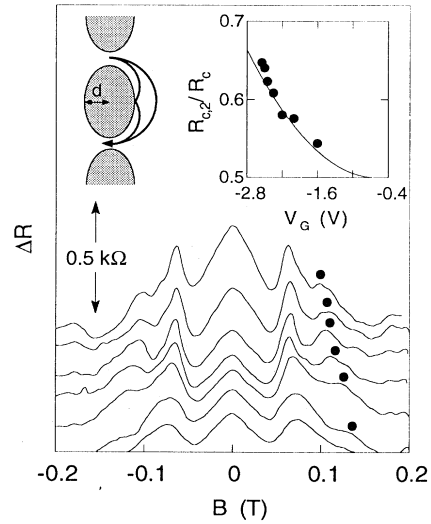

FIG. 5. Magnetoresistance of parallel point contacts (sample A) with optimized balance between both point contacts, taken at $T = 0.3$ K. Side gate voltages (in V) were $V_1 = -0.7$, $V_3 = -0.9$, and the center gate voltages were $= -1.6$, -2.0, -2.2, -2.35, -2.45, -2.50, and -2.55. Curves are offset on the resistance axis to accentuate the secondary reflection peaks (marked by dots) appearing on the shoulders of the primary focusing peaks. Inset: Ratio of secondary to primary peak position as a function of center gate voltage. The solid line is the quadratic fit discussed in the text.

trajectory similar to those seen in other experiments where electrons reflect specularly off a potential barrier.[2] Here, the secondary peak is due to the orbit in which the electron makes a single reflection off the antidot potential (see inset). The sharpness of the secondary peaks is dependent on the degree to which electrons are emitted directly out of the QPC, known as collimation, as well as the degree to which reflection is specular as opposed to diffuse. Normally, collimation is best accomplished when the width of the QPC is narrower, on the order of the Fermi wavelength. This is consistent with the increasing sharpness of the secondary peaks as the constrictions are narrowed.[1] As discussed previously, increasing the antidot voltage does not affect the primary peak position much because the electrons are chiefly emitted from the QPC center. However, the effective diameter of the potential antidot induced by the center gate increases with negative bias, so the focusing radius required to make a single reflection from this potential decreases.

We can quantify the behavior of the antidot potential by plotting the ratio of the primary peak position to the secondary peak potential as a function of antidot voltage, shown in the inset to Fig. 3. Since this ratio is also that of the secondary cyclotron radius R_{c2} to the primary radius R_c, we can fit it to a simple model of the geometry of the system, which assumes collimated electron emission, a single specular reflection from the antidot potential, and a linear relationship between the effective antidot radius d and the applied voltage, $R_{c2}/R_c = 0.5[1+(d/R_c)^2]$. The fit to the data yields $d/R_c = 0.25|V - V_{\mathrm{dep}}|$ with V in volts ($V_{\mathrm{dep}} = -0.6$ V is the depletion voltage); that is, d changes by 0.2 μm for every volt applied to the antidot ($R_c = 0.8$ μm), which is in good agreement with what we find in the conductance vs voltage dependence. Orbits consisting of additional reflections could not be observed, but the secondary peaks are further evidence of focusing in this system.

In conclusion, marked deviations from Ohm's law have been observed in the low-field magnetoresistance of closely spaced parallel QPC's. Though the low-field data for a single point contact can be closely matched to previously existing theory, the coupled system has transport features that cannot be explained by it. Rather, the features are consistent with cyclotron orbits reminiscent of those seen in antidot arrays. This is a demonstration of how transport anomalies related to classical focusing trajectories can be seen in a system consisting of a single antidot.

We acknowledge a helpful conversation with S. Goodnick. This work was supported by the U. S. DOE under Contract No. DE-AC04-94AL85000.

[1]For a review, see H. van Houten, C. W. J. Beenacker, and B. J. van Wees, in *Semiconductors and Semimetals,* edited by M. A. Reed (Academic, New York, 1989).

[2]H. van Houten *et al.*, Phys. Rev. B **39**, 8556 (1989).

[3]J. A. Simmons *et al.*, Phys. Rev. Lett. **63**, 1731 (1989); P. J. Simpson *et al.*, Surf. Sci. **305**, 453 (1994); C. J. B. Ford *et al.*, J. Phys. Condens. Matter **6**, L725 (1994).

[4]C. G. Smith *et al.*, J. Phys. Condens. Matter **1**, 6765 (1989); S. W. Hwang, J. A. Simmons, D. C. Tsui, and M. Shayegan, Phys. Rev. B **44**, 13 497 (1991).

[5]D. Weiss *et al.*, Phys. Rev. Lett. **66**, 2790 (1991).

[6]K. Nakamura *et al.*, Appl. Phys. Lett. **56**, 385 (1990); Y. Hirayama and T. Saku, Phys. Rev. B **42**, 11 408 (1990).

[7]M. E. Sherwin, J. A. Simmons, T. M. Eiles, N. E. Harff, and J. F. Klem, Appl. Phys. Lett. **65**, 2326 (1994).

[8]J. A. Nixon, J. H. Davies, and H. U. Baranger, Phys. Rev. B **43**, 12 638 (1991). The backscattering could be made worse by the relatively low density and corresponding poor screening in our samples.

[9]H. van Houten *et al.*, Phys. Rev. B **37**, 8534 (1988).

[10]S. E. Laux, D. J. Frank, and Frank Stern, Surf. Sci. **196**, 101 (1988).

[11]K.-F. Berggren, G. Roos, and H. van Houten, Phys. Rev. B **37**, 10 118 (1988).

[12]I. E. Aronov, M. Jonson, and A. M. Jagoskin, Phys. Rev. B **50**, 4590 (1994).

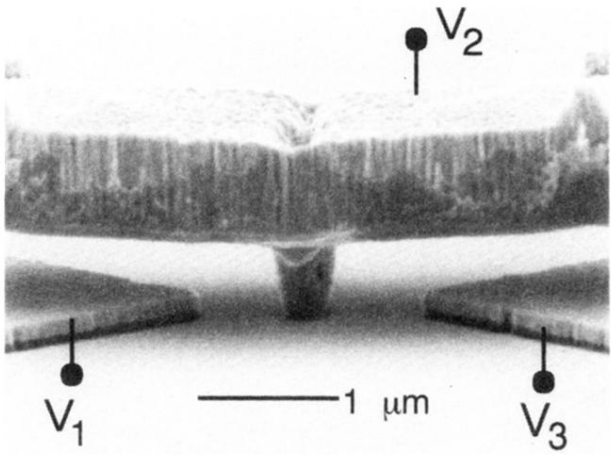

FIG. 1. SEM photograph of the airbridge structure and split gates used to define the two point contacts. Numbered voltages are applied to the gates as indicated. The lithographic width of the 2DEG channels on either side of the center gate is 0.8 μm.